Supplementary material for "Gyre dynamics modulate northward throughput of Gulf Stream water to subpolar latitudes"

Authors: Helene Asbjørnsen, Lea Svendsen, Yanchun He, Tillys Petit

Contents of this file: Figure S1, Figure S2, Figure S3, Figure S4, Figure S5, Figure S6, Figure S7

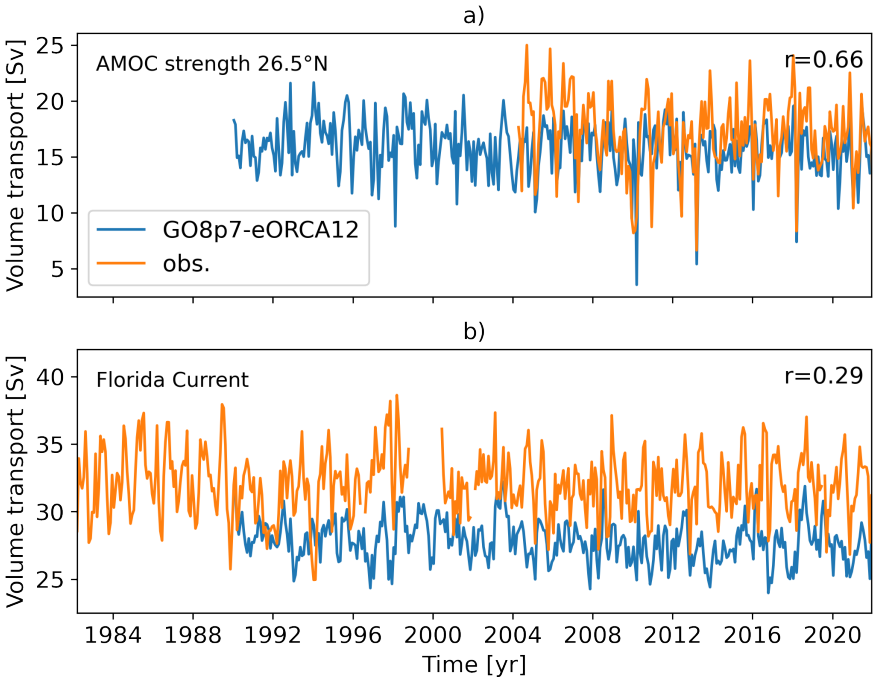

Fig. S1 Comparison with observations. (a) Monthly mean overturning strength in the GO8p7-eORCA12 hindcast at 26.5°N (Jan. 1990 - Dec. 2021) and the overturning strength measured at the RAPID array (Apr. 2004 - Dec. 2021). The overturning strength is here the maximum of the depth-space overturning stream function. (b) Monthly mean Florida Current volume transport in the GO8p7-eORCA12 hindcast at 26.5°N (Jan. 1990 - Dec. 2021) and the Florida Current volume transport from cable measurements in the Florida Straits (Mar. 1982 - Dec. 2021).

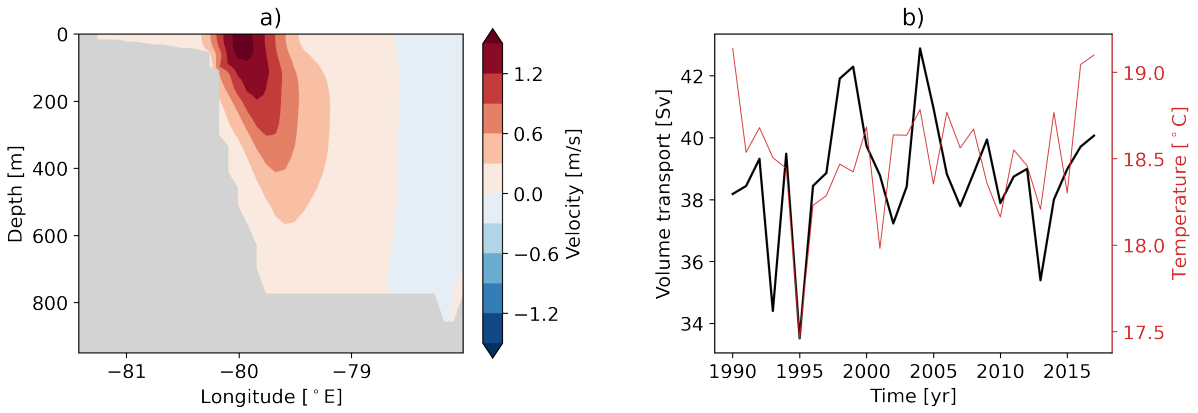

Fig. S2 Seeding section at 30°N. (a) Time mean meridional velocity at the 30°N particle seeding section. Particles are seeded monthly during 1990-2017 in all grid cells with a positive meridional velocity. (b) Annual mean Gulf Stream volume transport (northward velocities only) at the seeding section during 1990-2017 (black line; left axis). Annual mean temperature of the Gulf Stream water at the seeding section during 1990-2017 (thin red line; right axis). The time average volume transport is 38.7 ± 2.0 Sv, while the time average temperature is 18.5 ± 0.3 °C.

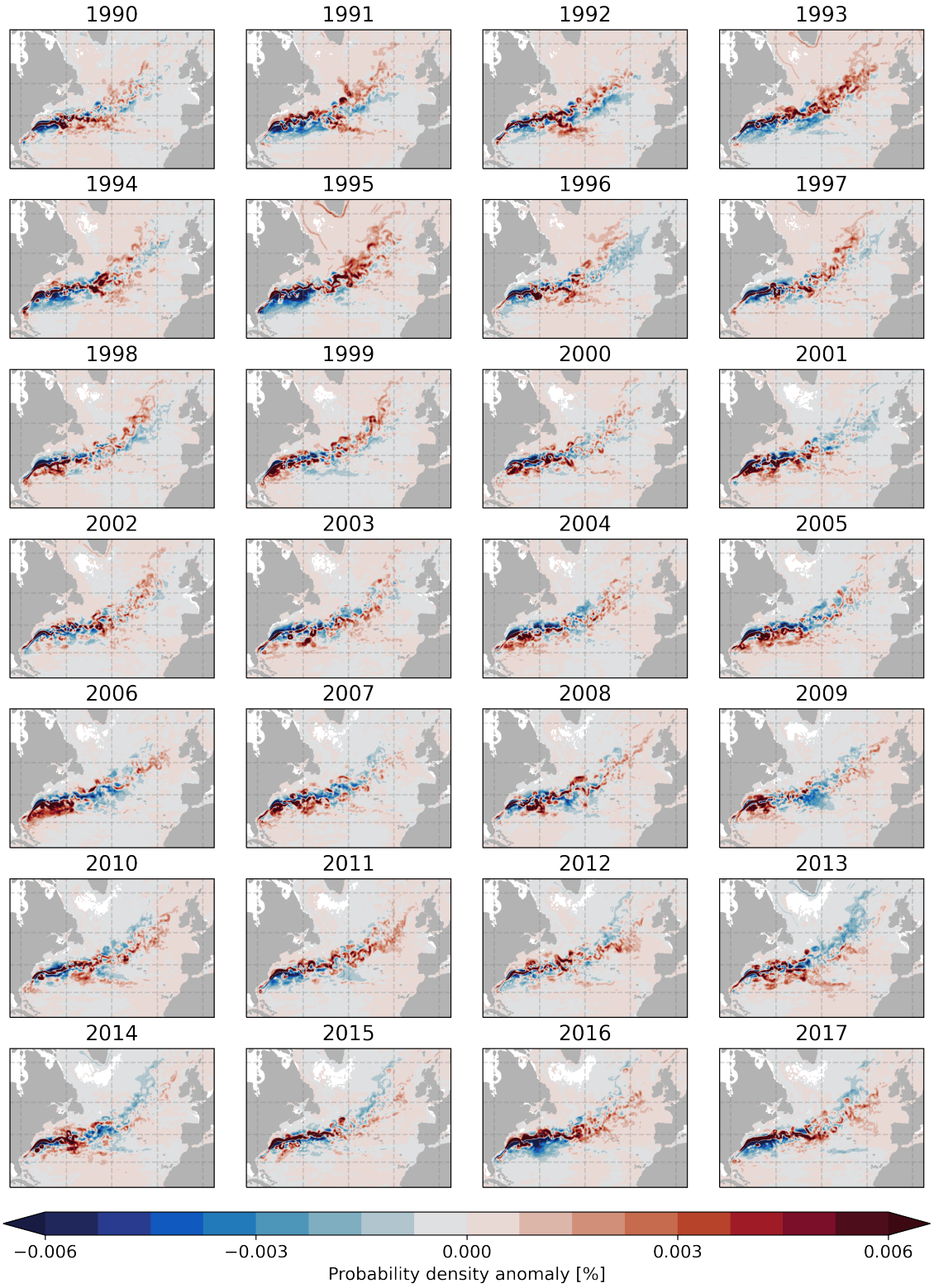

Fig. S3 Particle probability density anomaly. Anomaly from the mean volume weighted probability density distribution (seen in Figure 1b) for each seeding year between 1990 and 2017.

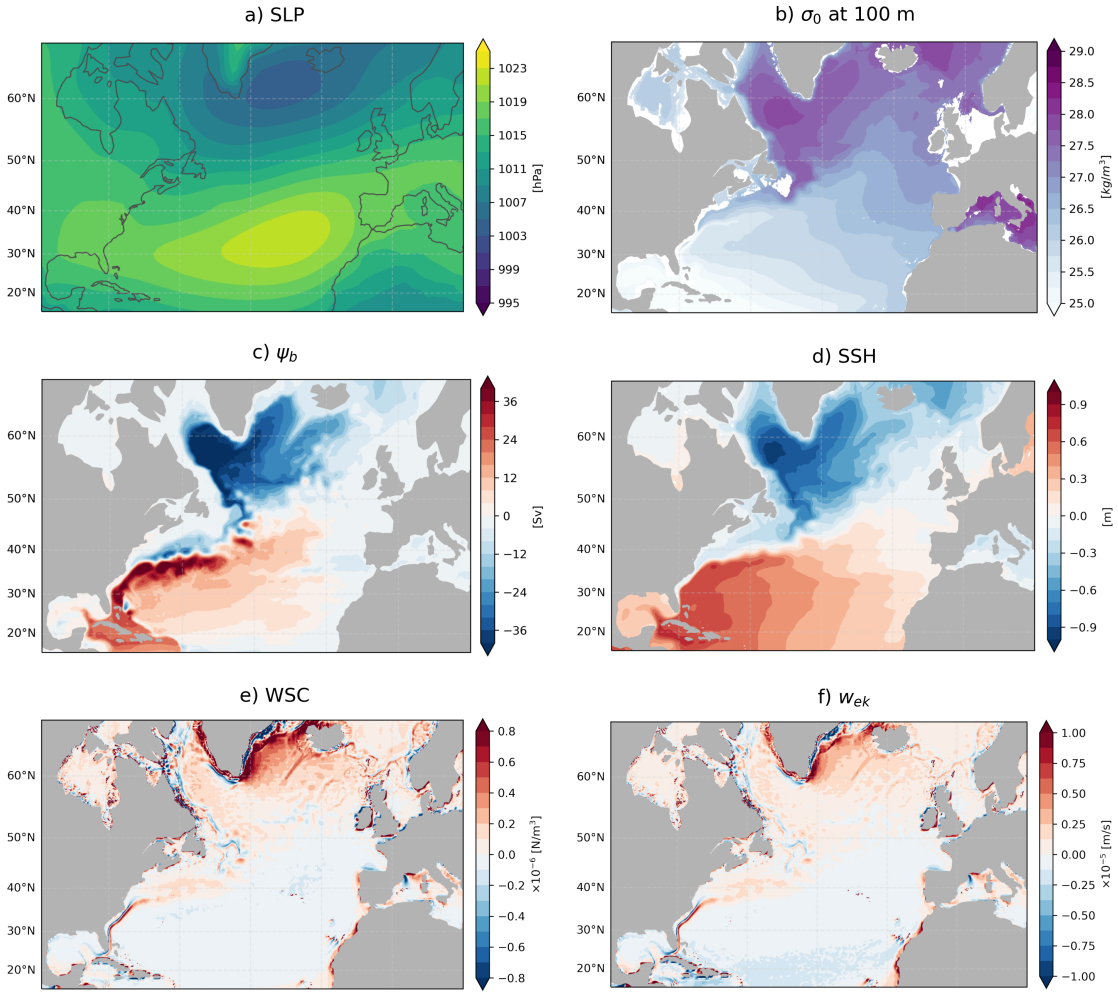

Fig. S4 Climatological fields for the 1990-2021 period. (a) Sea level pressure in hectopascal ('SLP'; hPa), (b) Potential density at 100m depth in kilogram per cubic meter ('σ_0'; kg/m^3). (c) Barotropic streamfunction in Sverdrup ('ψ_b'; Sv). (d) Sea surface height in meter ('SSH'; m). (e) Wind stress curl in Newton per cubic meter ('WSC'; N/m^3). (f) Vertical Ekman velocity in meter per second ('w_{ek}'; m/s; positive upward).

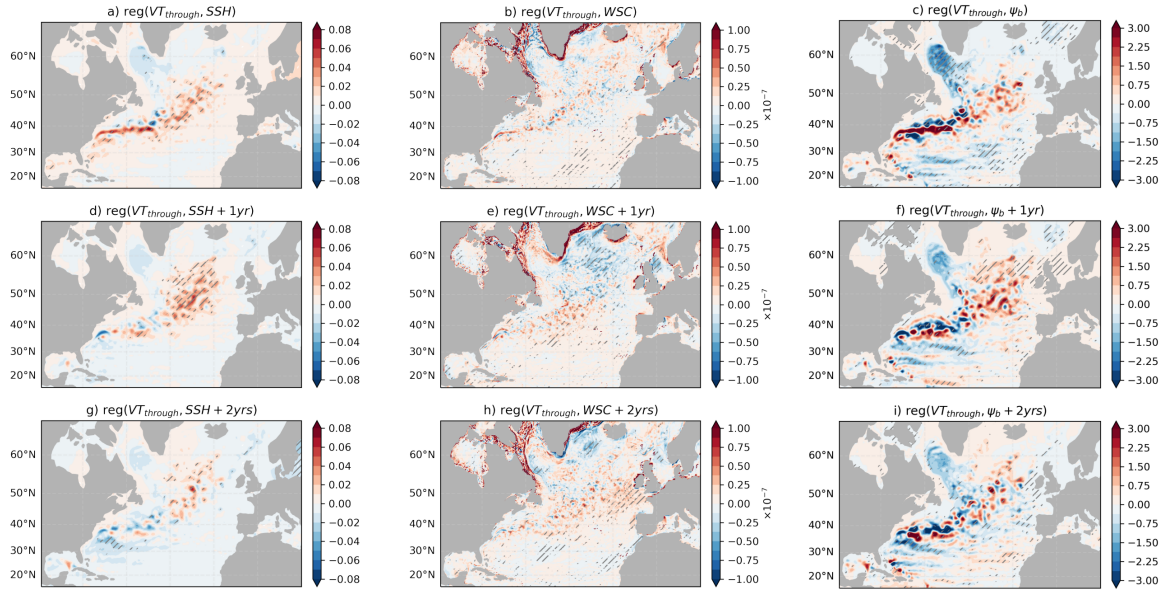

Fig. S5 Throughput variability and large-scale patterns in sea surface height, wind stress curl, and barotropic stream function. (a,d,g) Annual mean sea surface height ('SSH'; m) regressed onto the annual mean throughput time series ('through'; Sv). The unit is m per standard deviation of volume transport. (b,e,h) Annual mean wind stress curl ('WSC', N/m^3) regressed onto the annual mean throughput time series ('through'; Sv). The unit is N/m^3 per standard deviation of volume transport. (c,f,i) Annual mean barotropic streamfunction ('ψ_b', Sv) regressed onto the annual mean throughput time series ('through'; Sv). The unit is Sv per standard deviation of volume transport. Because the throughput time series is sorted by the seeding year at 30°N and the particles typically use between three months to two years to reach 45°N, we show the regression at zero lag (a-c), SSH, WSC, ψ_b lagging with one year (d-f), and SSH, WSC, ψ_b lagging with two years (g-i). (a-i) Significance at the 90% confidence level is indicated in hatching.

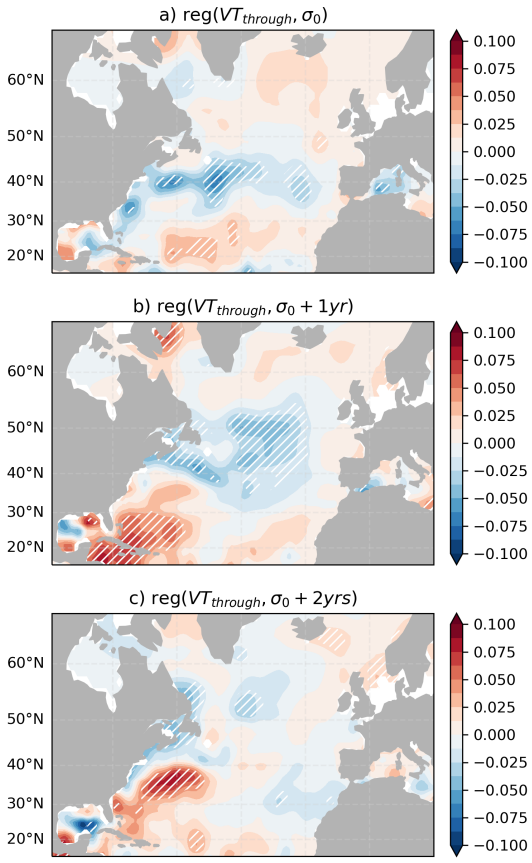

Fig. S6 Throughput variability and large-scale patterns in observed subsurface densities. Annual mean potential density at 100 m depth ('σ_0'; kg/m^3) from the EN4.2.2 gridded observational product regressed onto the annual mean throughput time series ('through'; Sv). The throughput time series has been standardized and the unit is kg/m^3 per standard deviation of volume transport. Significance at the 90% confidence level is indicated in hatching.

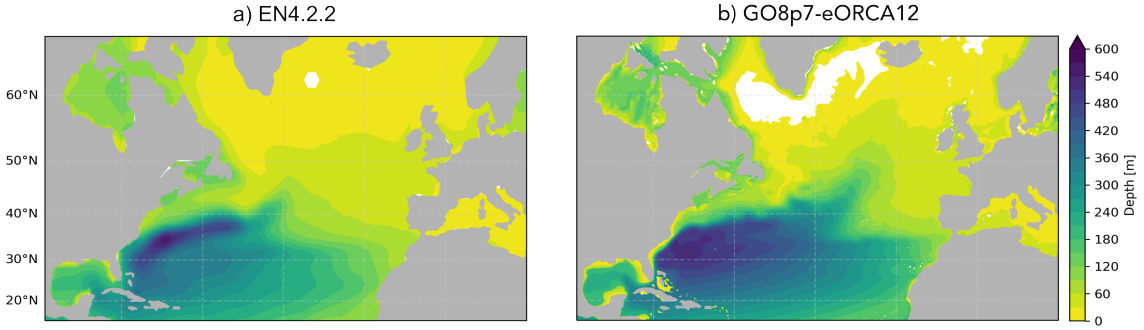

Fig. S7 Depth of the $\sigma_0 = 26.5\ kg/m^3$ isopycnal averaged over the 1990-2021 period in (a) the EN4.2.2 gridded observational product and in (b) the GO8p7-eORCA12 ocean hindcast.